AGU PUBLICATIONS

Supporting Information for "Flood variability determines the location of lobe-scale avulsions on deltas: Madagascar"

Sam A. S. Brooke[1], Vamsi Ganti[1,2], Austin J. Chadwick[3], Michael P. Lamb[4]

[1]Department of Geography, University of California Santa Barbara, Santa Barbara, CA 93106, USA
[2]Department of Earth Science, University of California Santa Barbara, Santa Barbara, CA 93106, USA
[3]University of Minnesota, Department of Earth Sciences and St. Anthony Falls Laboratory, 2 Third Ave. SE, Minneapolis, Minnesota, USA
[4]Division of Geological and Planetary Sciences, California Institute of Technology, Pasadena, CA 91125, USA

Contents of this file

1. Text S1 to S5

2. Figures S1 to S7

Additional Supporting Information (Files separate)

1. Captions for large Tables S1 to S2 (separate files)

Corresponding author: S. A. S. Brooke, Department of Geography, University of California Santa Barbara, 4812 Ellison Hall, Santa Barbara, CA 93106, USA. (sbrooke@ucsb.edu)

Introduction

The supplementary information file contains the following:

1. Details about the estimation of the backwater and drawdown lengths for the Madagascan rivers (text S1).

2. Derivation of the flood-scour length relation (text S2), which was originally derived for sand-bedded rivers (Ganti et al., 2019) and extended here to include silt-bedded rivers.

3. Methods used to estimate the bankfull flow depth of the Madagascan rivers (text S3).

4. Details about the location of lobe-scale avulsions on the western coast of Madagascar (text S4).

5. Details about how we incorporated uncertainties and performed error propagation when evaluating $\overline{L_b}$ and l_{scour} (text S5).

6. Additional supporting figures (Figures S1–S7) and supplementary tables (Table S1 and S2) with data generated in this study.

Text S1. – Computation of the backwater and drawdown length

For a rectangular channel, the analytical solution for the upstream distance from the river mouth that is affected by backwater or drawdown is given by (Bresse, 1860):

$$\frac{L_b}{\overline{L_b}} = \frac{h_c}{h_n} \times \left(\zeta_s - \zeta_l - \left(1 - Fr^2\right)\left(Z(\zeta_s) - Z(\zeta_l)\right)\right) \tag{1}$$

where L_b is the backwater or drawdown length, $\overline{L_b}$ is the backwater lengthscale, $\zeta_s = h_s/h_n$, $\zeta_l = 0.95$, Fr is the Froude number, h_s and h_n are the flow depth at the river mouth and the normal-flow depth for a given flood, h_c is the bankfull flow depth in the normal-flow reach, and $Z(\zeta)$ is a function given by:

$$Z\left(\zeta\right) = \frac{1}{6}\ln\left(\frac{\zeta^2 + \zeta + 1}{\left(\zeta - 1\right)^2}\right) - \frac{1}{\sqrt{3}}\arctan\left(\frac{\sqrt{3}}{2\zeta + 1}\right) \tag{2}$$

For the Madagascan rivers, we assumed that the flow depth at the river mouth is equal to the bankfull flow depth, i.e., $h_s = h_c$. To compute the drawdown length, we set $h_n = 3h_c$, consistent with global compilation of alluvial rivers (Gibling, 2006; Ganti et al., 2014). To comupte the backwater length, we set $\frac{h_s}{h_n} = \left(\frac{Q_{bf}}{Q_{low}}\right)^{2/3}$ following the Manning-Strickler relation, where Q_{bf} is the bankfull water discharge and Q_{low} is the lowest discharge in monthly discharge record for the Madagascar rivers. Depth-averaged flow velocity measurements on the Mangoky river indicate that $Fr \approx 0.3$. Evaluation of equations (1) and (2) indicated that (a) the backwater length is $0.98\overline{L_b}$, and b) the drawdown length is $1.3\overline{L_b}$ — distances that were significantly shorter than the measured avulsion length (Fig. 3a in main text).

Text S2. – Flood scour length (l_{scour}) derivation

The starting point for the analysis is the expression for the dimensionless flood scour length as described in Ganti et al. (2019):

$$\frac{l_{scour}}{\overline{L_b}} = \sqrt{\frac{t_{scour}}{t_{adj}}} \tag{3}$$

where t_{adj} is the bed adjustment timescale and t_{scour} is the typical flood duration. The bed adjustment timescale is (Chatanantavet and Lamb, 2014):

$$t_{adj} = \frac{h_c \overline{L_b}}{q_s} \tag{4}$$

where h_c is the bankfull flow depth and q_s is the volumetric unit sediment flux. We computed q_s using (Ma et al., 2017; 2020):

$$q_s = q_s^* \sqrt{RgD_{50}^3} \tag{5}$$

where D_{50} is the median bed-material grain size, R is submerged specific gravity of sediment (1.65 for quartz), g is the acceleration due to gravity, and

$$q_s^* = \frac{\alpha \tau^{*n}}{C_f} \tag{6}$$

where τ^* is a dimensionless bed shear stress, C_f is a dimensionless friction factor, and α and n are grain-size-dependent constants, given by:

$$\alpha(D_{50}) = \frac{0.859}{1 + exp[10^5(D_{50} - 1.6 \times 10^{-4})]} + 0.036 \tag{7}$$

$$n(D_{50}) = \frac{1.322}{1 + exp[10^5(-D_{50} + 1.6 \times 10^{-4})]} + 1.678 \tag{8}$$

Substituting (5) into (4) and rearranging (3) results in:

$$\frac{l_{scour}}{\overline{L_b}} = \left[t_{scour} \frac{\sqrt{RgD_{50}^3}\alpha(h_n S)^n}{h_c \overline{L_b} C_f (RD_{50})^n} \right]^{0.5} \tag{9}$$

where h_n is the normal-flow depth during a typical flood.

Text S3. – Channel depth estimation

For Madagascan rivers, we estimated the bankfull flow depth (h_c) using two independent methods. First, we calculated h_c using the threshold-channel theory for alluvial rivers (Dunne and Jerolmack, 2018):

$$h_c = \frac{1.2\tau_c}{\rho g S} \tag{10}$$

where τ_c is the bank shear stress, set to vary uniformly between 6-10 Pa, consistent with global alluvial river compilation, ρ is the density of water (1000 kg/m^3) and S is channel bed slope, measured from elevation profiles (Figs. S5 & S1). Second, we independently estimated h_c using the empirical bankfull Shields stress criterion proposed by Trampush et al. (2014) using $D_{50} = 90\mu m$.

Text S4. – Location of fan avulsions

We observed two lobe-scale fan avulsions on the Betsiboka and Mahajamba rivers, 169 km and 198 km upstream from the shoreline, respectively (Fig. S7). Unlike the five lobe-scale delta avulsions discussed in the main text, these avulsion sites are downstream of an abrupt channel-gradient break (Fig. S7), corresponding with a loss in valley confinement. Across the avulsion site, the median channel-bed slope (first and third quartiles) decreases from 3.6×10^{-3} (2.4×10^{-3} and 6.4×10^{-3}) to 1.2×10^{-3} (8.0×10^{-4} and 1.3×10^{-3})

for the Betsiboka River—a threefold decrease (Fig. S7). Similarly, for the Mahajamba River, the slope decreases from 3.4×10^{-3} (2.9×10^{-3} and 8.2×10^{-3}) to 1.0×10^{-3} (5.6×10^{-4} and 1.2×10^{-3})—an 3.4 factor decrease (Fig. S7). Our results suggest that these topographic changes result in approximately an 18-fold and 16-fold decrease in the volumetric sediment transport capacity (equation 5) for the Betsiboka and Mahajamba rivers, respectively, across their avulsion sites. These observations are consistent with the bed-slope mediated avulsion model for fans (Ganti et al., 2014), where abrupt topographic changes cause a drop in the sediment-transport capacity that drives sedimentation and subsequent avulsion (Jones and Schumm, 1999; Slingerland and Smith, 2004; Hartley et al., 2017). A similar decline in channel gradient and sediment-transport capacity were documented for the lobe-scale fan avulsions on the Huanghe (Ganti et al., 2014).

Text S5. – Incorporation of uncertainty and error propagation

In this section, we describe how we incorporated uncertainty and propagated error in the estimation of $\overline{L_b}$ and l_{scour}. In all cases, we used Monte Carlo simulation for error propagation where each parameter's uncertainty was assigned a given distribution (as described below) and we generated 20,000 independent samples for every parameter value. To estimate $\overline{L_b}$ with error, we needed to incorporate the uncertainty associated with the estimation of h_c and S, which was done as follows:

S: We incorporated the uncertainty in S by including the spread of the values of topographic slope within 5 km spatial windows, binned every 25 km. For all Madagascan rivers, we generated uniformly distributed S values, with the distribution centered at the estimated median value and the width of the distribution equal to the estimated interquartile range. Local measurements of slope had a skewed distribution with outliers, and we characterized the central tendency and spread of the data using the median and interquartile range as opposed to mean and standard deviation, respectively.

$\mathbf{h_c}$: For the Madagascan rivers, we estimated h_c using the empirical methods of Trampush et al. (2014) and Dunne and Jerolmack (2018) as outlined in Text S3. Both these methods have their own associated uncertainty and to represent the entire spread of possible h_c values, we randomly chose h_c from either of the pools of possible values of h_c with equal likelihood. This ensured that our Monte Carlo sampling covered the entire range of possible values expected under the empirical relations of Trampush et al. (2014) and Dunne and Jerolmack (2018), together with their associated errors.

For all other low-gradient river deltas, the values of h_c and S were reported in previous studies (Jerolmack and Mohrig, 2007; Jerolmack and Swenson, 2007; Chatanantavet et al., 2012; Ganti et al., 2014; 2019; Moodie et al., 2019). To quantify the error on l_{scour}, we needed to further constrain the uncertainty associated with h_n, t_{scour}, and C_f (see equation (9)). The uncertainty of h_c and S were quantified as described above and other parameters (R, D_{50}, α, n) are deterministic.

$\mathbf{h_n}$: For all rivers considered in this study, we assumed the normal-flow depth of a typical flood to be uniformly distributed between $2h_c$ and $4h_c$ based on global compilation (Gibling 2006; Ganti et al. 2014).

$\mathbf{t_{scour}}$: The typical duration of a flood event was constrained using historical water discharge data. We assumed a normal distribution of t_{scour} values with mean and standard deviation equal to the estimated mean and standard error of the t_{scour} values from the historical discharge records. For the low-gradient river compilation and Mangoky, Morondava and Manambolo rivers, gauged data are available close to the avulsion sites; however, the discharge records for the Sambao and Fiherenana rivers were approximated using the closest gauge station (Betsiboka and Mangoky river stations, respectively, see Fig. S1). t_{scour} values for low-gradient and Madagascar rivers are compiled in table S2.

$\mathbf{C_f}$: We used the C_f values reported by previous authors for the low-gradient rivers. For the Madagascan rivers, we used the estimated value of the Mangoky river of $C_f \approx 0.01$, which is similar to the typical average value assumed for alluvial rivers globally (e.g., Dunne and Jerolmack, 2018).

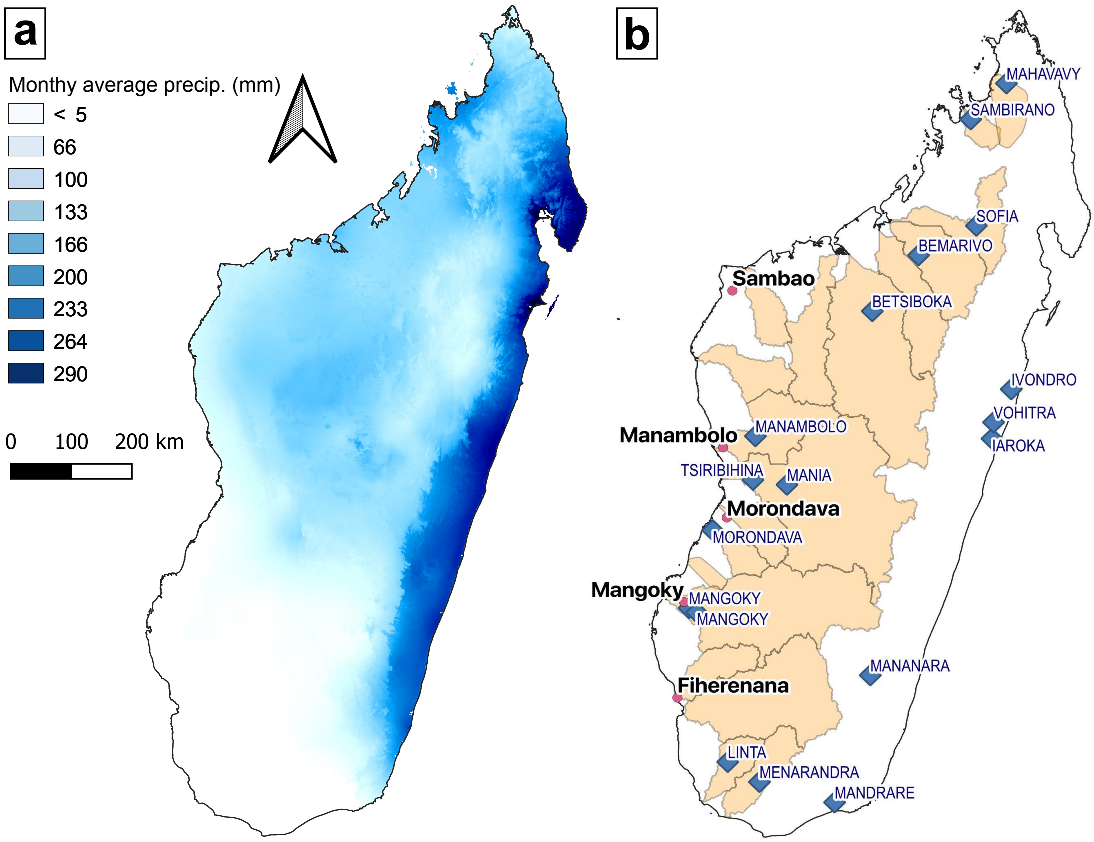

Figure S1. (a) Monthly-averaged precipitation generated from Worldclim2 interpolated weather station data (Fick and Hijimans, 2017), showing the major E-W and N-S precipitation gradients on the island of Madagascar. (b) Location of GRDC river discharge gauge stations across Madagascar relative to westerly draining river catchments. For rivers without gauges, the Fiherenana and Sambao rivers, flood scour durations (t_{scour}) were estimated from the proximal Mangoky and Betsiboka rivers, respectively.

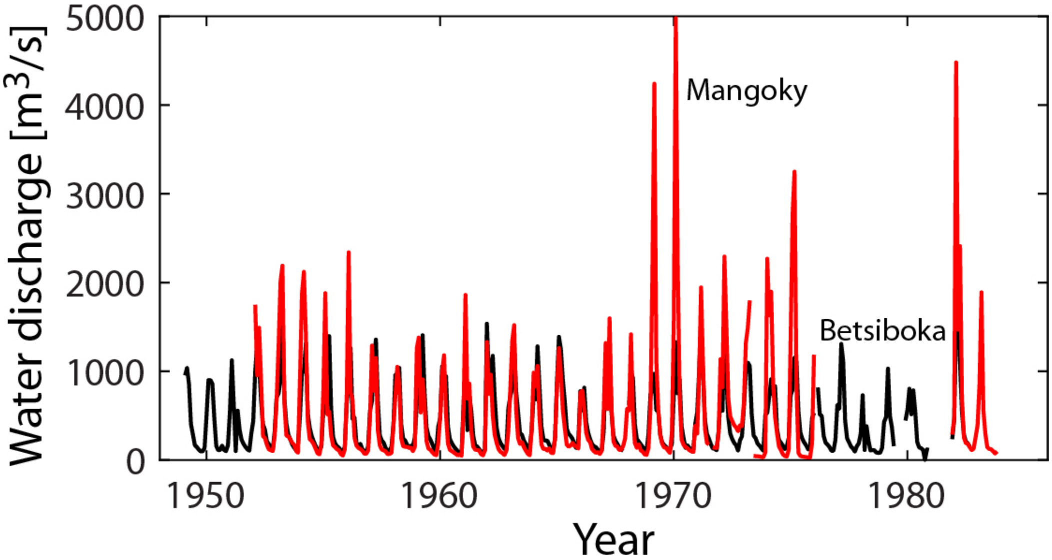

Figure S2. RivDis (Vorosmarty et al., 1998) discharge time series of the Mangoky and Betsiboka rivers in Madagascar.

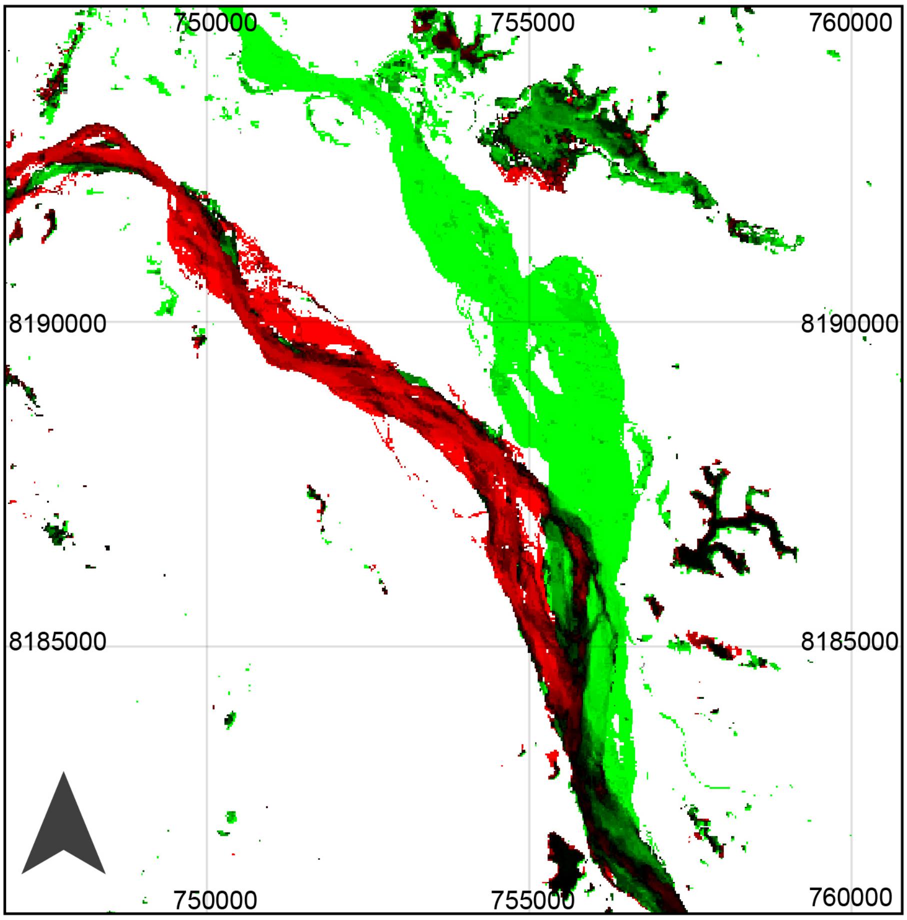

Figure S3. Example surface water mask from the European Commission's Joint Research Center Global Surface Water dataset (Pekel et al., 2016). Net surface water difference from 1984-2018 for the Mahajamba fan avulsion, with previously occupied channels in red and newly occupied channels in green.

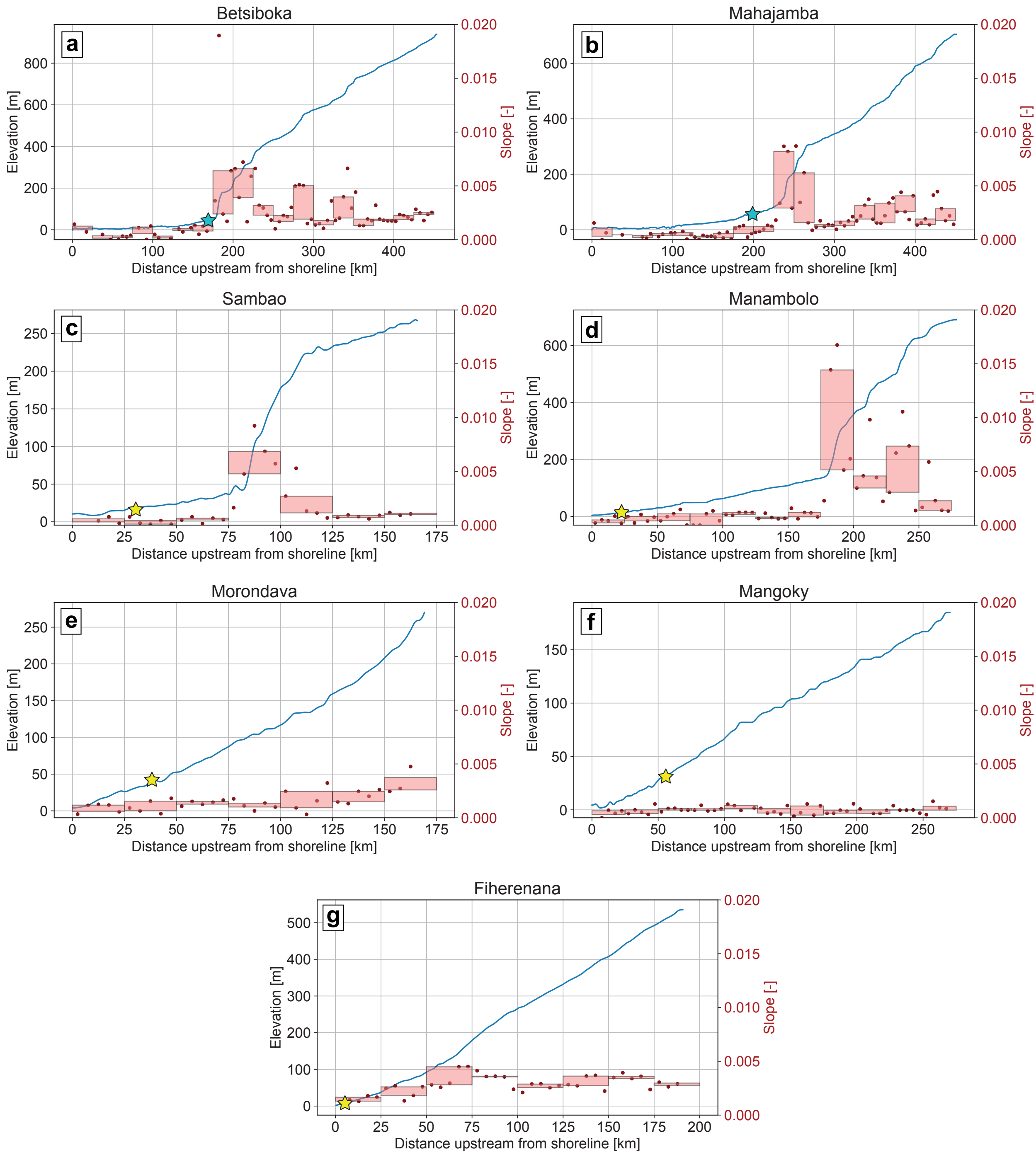

Figure S4. Long profiles of (a) Betsiboka and (b) Mahajamba rivers, where blue stars denote avulsion sites. Local slope was measured from elevation change every 5 km (red dots), and binned into 25 km segments. The translucent boxes denote the interquartile range of slopes, measured within each bin. (c-g) Long profiles of rivers with lobe-scale delta avulsions, where yellow stars denote avulsion sites. Note that, unlike fan avulsions, there is no distinctive channel-gradient break across the delta avulsion sites.

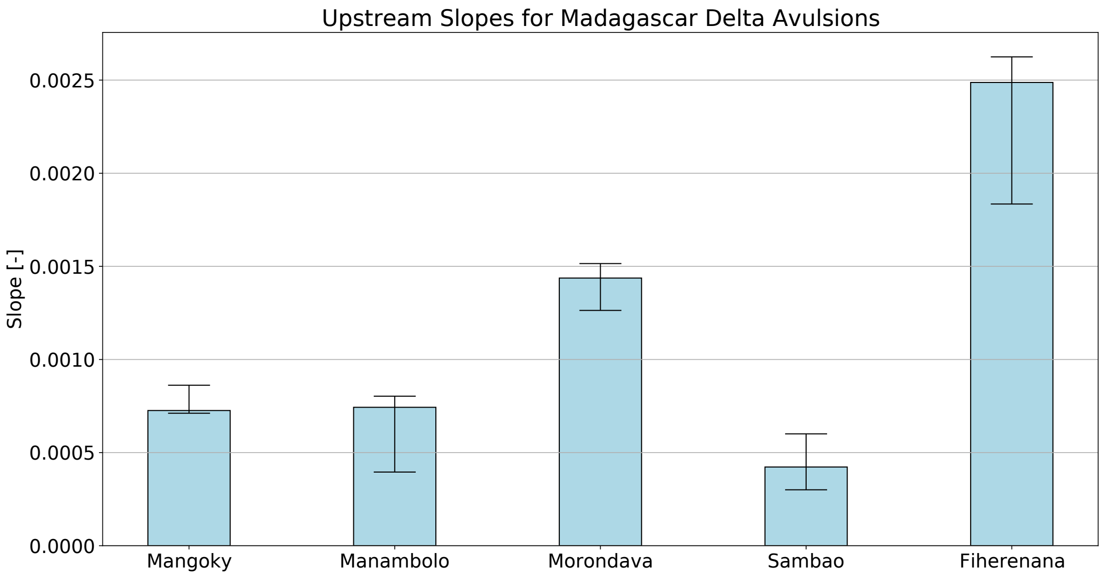

Figure S5. Bar plot of the estimated median slopes of the Madagascan rivers on which we observed lobe-scale delta avulsions. Estimated slopes were from the 25 km bin immediately upstream of the observed avulsion sites. Error bars show the interquartile range.

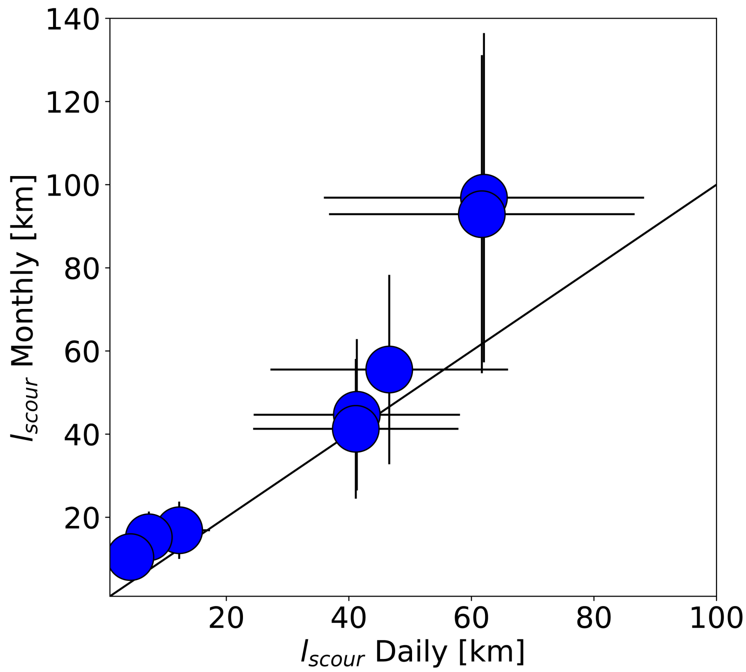

Figure S6. Estimated flood-scour length for rivers from the global delta avulsion length compilation, where both monthly and daily discharge data were available. The solid black line indicates 1:1 line, and the error bars denote the standard deviation resulting from our Monte Carlo simulation approach to quantifying error on l_{scour}.

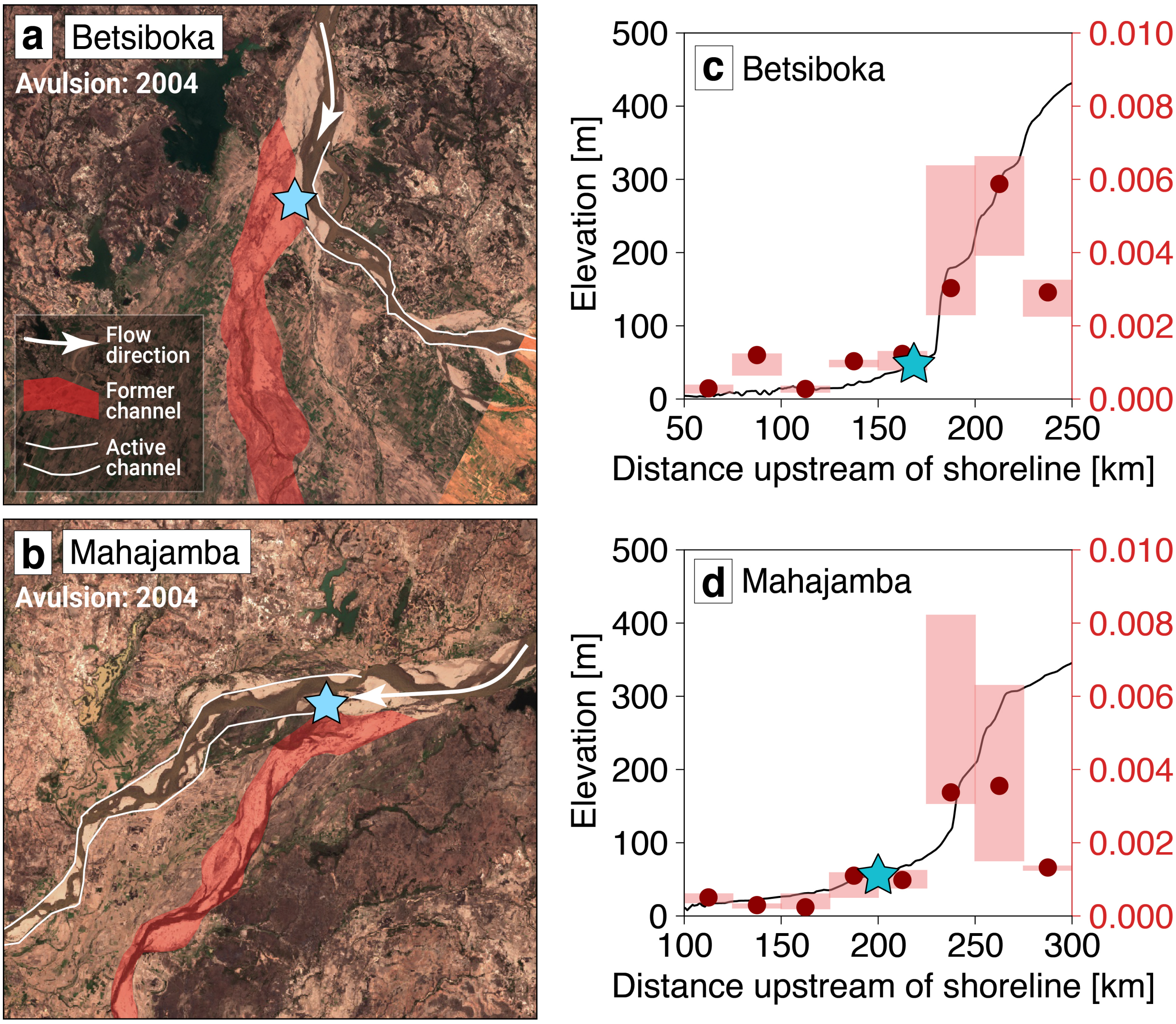

Figure S7. Location of lobe-scale fan avulsion sites in Madagascar. (a, b) ESA Sentinel 2 bottom-of-atmosphere-corrected optical imagery of avulsion sites on Betsiboka and Mahajamba rivers (blue stars). Right-to-left flow direction long profiles (black lines) of the (c) Betsiboka and (d) Mahajamba rivers, extracted from the 30 m resolution SRTM data. Measured median slopes (red markers), along with their interquartile range (translucent red bar), at 5 km intervals binned into 25 km non-overlapping windows (right y-axis). Blue stars indicate avulsion sites.

Table S1. Source discharge data for each river with delta avulsions, where bankfull discharge (Q_{bf}) is estimated from the median of interannual peak dischages ($Q_{bf} - Estimated$) or taken from reported values ($Q_{bf} - Reported$), when available. For each river we estimate t_{scour} as the mean duration of time intervals (flood events) where Q_{bf} is exceeded.

Table S2. Full set of parameters for calculating flood scour length (l_{scour}) for global compilation and Madagascar deltas.